An Effective Model for Microscopic Intrinsic Localized Modes.

G. Kalosakas and A. R. Bishop

Theoretical Division and Center for Nonlinear Studies,
Los Alamos National Laboratory, Los Alamos, NM 87545

ABSTRACT

We present a system of coupled degrees of freedom that can effectively describe the localization of intramolecular excitations in the charge transfer solid $PtCl$. These excitations correspond to the Raman active motion of chlorines (symmetric $Pt-Cl$ stretching). By fitting two parameters of the model we obtain an accurate description of the strong red-shifts that appear in the overtone Raman spectra of the isotopically pure material. The resulting intrinsic localized modes extend on length scales of the order of nanometers. With the same set of parameters the model can reproduce the specific structure of the Raman spectra of naturally abundant $PtCl$, which contains a random distribution of chloride isotopes.

Keywords: Intrinsic localized modes, breathers, overtone red-shifts, isotopic disorder, $PtCl$ Raman spectra.

1 INTRODUCTION

The resonance Raman spectra of both naturally abundant and isotopically pure $PtCl$ constitute a direct indication of microscopic vibrational intrinsic localized modes (ILMs) in a solid [1]. The abbreviation $PtCl$ represents the halogen bridged, mixed valence, transition metal compound $\{[Pt(en)_2][Pt(en)_2Cl_2](ClO_4)_4\}$, where $en =$ ethylenediamine (see for example reference [2]). The unit cell of this quasi one-dimensional solid contains the molecular unit $Cl^- - Pt^{+4} - Cl^- \cdots Pt^{+2}$, where two en ligands are chemically bonded to each Pt ion. $PtCl$ is a strong charge density wave material with highly nonlinear properties [2]–[4].

1.1 The Model

We use a Holstein-type Hamiltonian [5], [6] to model the interactions of intramolecular excitations corresponding to the symmetric vibration of the chlorides within a unit cell. In particular [7], [8],

$$H = H_{exc} + H_{env} + H_{int}, \tag{1}$$

where the first term represents a tight-binding approximation for the intramolecular excitations,

$$H_{exc} = \sum_i \left(E_0 \alpha_i^\dagger \alpha_i - J(\alpha_i^\dagger \alpha_{i+1} + \alpha_{i+1}^\dagger \alpha_i) \right), \tag{2}$$

the second term describes an interactive environment represented by classical Einstein oscillators,

$$H_{env} = \sum_i \frac{p_i^2}{2M} + \sum_i \frac{M\omega_0^2}{2} x_i^2, \tag{3}$$

and the last term corresponds to a linear coupling

$$H_{int} = \chi \sum_i x_i \alpha_i^\dagger \alpha_i. \tag{4}$$

In eq. (2) the $\alpha_i^\dagger$ and α_i are creation and annihilation operators, respectively, of intramolecular excitations on lattice site i. The on-site energy of the excitation is E_0 and J is the transfer integral between adjacent sites. In eq. (3) x_i and p_i are the displacement from the equilibrium position and the momentum, respectively, of the i^{th} oscillator. Each oscillator has mass M and frequency ω_0. Finally, in eq. (4) χ is the strength of the interaction between the coupled degrees of freedom.

2 RED-SHIFTS OF ISOTOPICALLY PURE MATERIAL

2.1 Many-Quanta Stationary States

Using J as the unit of energy and dimensionless parameters [6], we obtain that in the adiabatic approximation the stationary solutions of Hamiltonian (1) depend on two parameters: the dimensionless on-site energy $\epsilon_0 = E_0/J$ and the dimensionless coupling constant $k = \chi/\sqrt{JM\omega_0^2}$. In that case the eigenvalue equation of a general N-quanta stationary state is given by [7]:

$$E\Phi_{j_1,j_2,\ldots,j_N} = (N\epsilon_0 - \Delta_N - k^2 P_N)\Phi_{j_1,j_2,\ldots,j_N}, \tag{5}$$

where $E = E_{exc} + E_{int}$ and $\Phi_{j_1,j_2,\ldots,j_N}$ is the time independent probability amplitude for finding one intramolecular quantum on site j_1, one on site j_2, etc. Furthermore, in the last equation

$$\Delta_N \Phi_{j_1,\ldots,j_N} = \sum_{n_{j_1}} \Phi_{n_{j_1},\ldots,j_N} + \ldots + \sum_{n_{j_N}} \Phi_{j_1,\ldots,n_{j_N}}, \quad (6)$$

where the indices n_{j_i} denote summation over the nearest neighbors of site j_i, and

$$P_N = N \sum_{j=j_1,\ldots,j_N} \left(\sum_{i_1,\ldots,i_{N-1}=1}^{L} |\Phi_{j,i_1,\ldots,i_{N-1}}|^2 \right), \quad (7)$$

where L is the number of lattice sites.

The eigenvalue equation (5) admits extended (Bloch type) solutions which form a band extending from $N(\epsilon_0 - 2)$ to $N(\epsilon_0 + 2)$ in the limit of infinite chain. Additionally, localized modes below this band exist, due to the nonlinearity.

2.2 Numerical Calculation of the Ground State

A simple numerical method for the calculation of the N-quanta ground state of eq. (5) results from the fact that it constitutes an attractor of the map

$$\{\Phi\} \longrightarrow \frac{\mathcal{H}\{\Phi\}}{\|\mathcal{H}\{\Phi\}\|},$$

where $\{\Phi\} = \{\Phi_{j_1,\ldots,j_N},\ j_1,\ldots,j_N, = 1,\ldots,L\}$. The operator $\mathcal{H}$ defined as minus the right hand side of eq. (5) and $\|\mathcal{H}\{\Phi\}\|$ is the norm of the vector $\mathcal{H}\{\Phi\}$ (for more details see reference [6]).

In order to calculate the ground state for a particular number of quanta, N, we begin with an initial state completely localized at one lattice site, say n_0,

$$\Phi^{init}_{j_1,\ldots,j_N} = \delta_{j_1,n_0} \cdots \delta_{j_N,n_0},$$

act on this with the operator $\mathcal{H}$, normalize the resulting vector and repeat this procedure until convergence is achieved. At the end we find the wavefunction $\{\Phi^{final}\}$, while the energy E of eq. (5) is given through the norm $\|\mathcal{H}\{\Phi^{final}\}\|$. Then, the total energy E_N obtained by the inclusion of the E_{env} of eq. (3) [1]. This procedure converges rapidly to the localized ground state.

As N increases, the resulting ground states characterized by the increasing of the absolute value of the binding energy (referring to the lower band edge of the extended N-quanta stationary states) and the stronger localization of the wavefunction [7].

[1] In the adiabatic approximation $p_i = 0$ and the x_i are given in terms of the resulting wavefunction Φ^{final} [7].

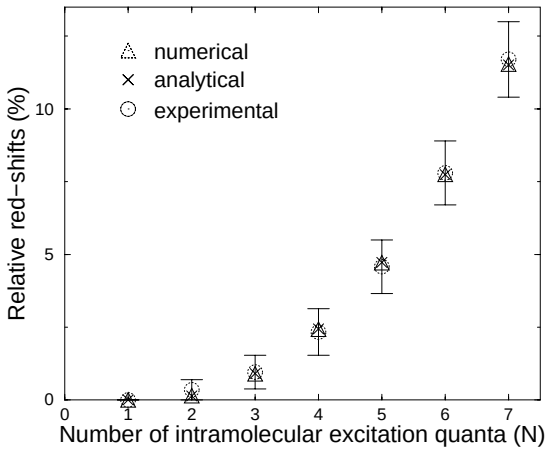

Figure 1: Relative red-shifts of the $Pt^{35}Cl$ overtone Raman spectra as a function of the number of excitation quanta, N. The error bars represent experimental errors.

2.3 Parameter Values

The increase of the binding energy results in strong red-shifts in the overtone spectra. The fitted values

$$k = 1.2\ \ (\pm 0.1)\ \text{ and }\ \epsilon_0 = 200\ \ (\pm 30) \quad (8)$$

provide accurate agreement with the corresponding experimental red-shifts of the overtone Raman spectra, for both $Pt^{35}Cl$ and $Pt^{37}Cl$. In figure 1 we show the numerical relative red-shifts for up to the $N = 7$ quanta (sixth overtone) for the case of $Pt^{35}Cl$, along with the experimental data of reference [1]. Analytical results are also available through accurate approximate expressions [7].

The experimental values of the fundamental frequencies are 312 cm^{-1} for $Pt^{35}Cl$ and 304 cm^{-1} for $Pt^{37}Cl$ [1]. For values of k below ~ 1.5 the energy of the single quantum ground state of Hamiltonian (1) is approximately obtained by $\epsilon_0 - 2$ [6]. As a result we have that

$$\text{for } Pt^{35}Cl: \ J \approx 1.58\ cm^{-1} \text{ and } E_0 \approx 315\ cm^{-1}, \quad (9)$$

and

$$\text{for } Pt^{37}Cl: \ J \approx 1.54\ cm^{-1} \text{ and } E_0 \approx 307\ cm^{-1}. \quad (10)$$

The fitted values of the parameters, eqs. (8) and (9), (10), are consistent with independent calculations arising from physically different properties of the material [8], viz. the position and the width of the relevant phonon dispersion branch ν_1 and the requirement that the nonlinearity of the effective model mimics the lattice anharmonicity induced by the underlying electron-phonon interacting system that is actually responsible for the formation of the ILMs.

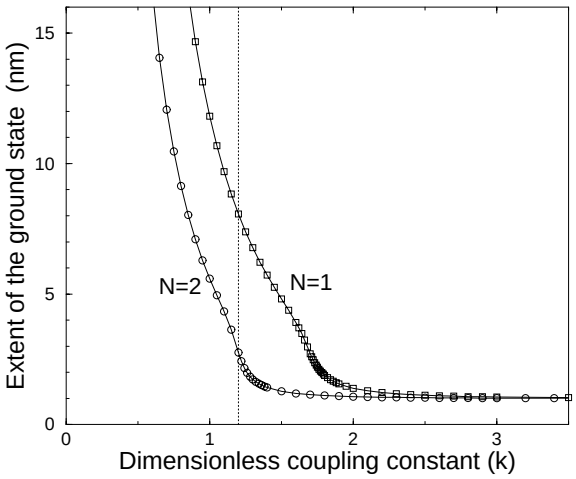

Figure 2: The extent of the 1-quantum and 2-quanta ground state as a function of k. The dotted line denotes the fitted value of k for $PtCl$.

The ground state wavefunction depends only on the value of the dimensionless coupling k. In figure 2 we plot the variation of the extent of the wavefunction for $N = 1$ and $N = 2$ with k. The extent is calculated through the participation number [9], Z, of the corresponding solution, where $Z = 1/\sum_{j=1}^{L} |\Phi_j|^4$ for $N = 1$ and $Z = 1/\sum_{j_1,j_2=1}^{L} |\Phi_{j_1,j_2}|^4$ for $N = 2$, respectively, and the use of the value of $PtCl$'s lattice constant which is equal to 1.08 nm. The fitted value of $k = 1.2$ for the $PtCl$ indicates that a single quantum ILM extends over about 8 nm, while a 2-quanta ILM extends over $2 - 3$ nm.

3 RAMAN SPECTRA OF NATURALLY ABUNDANT MATERIAL

The natural abundance of Cl consists of 75.6% ^{35}Cl and 24.4% ^{37}Cl. As a result the naturally abundant $PtCl$ contains 57.2% unit cells with $^{35}Cl-^{35}Cl$, 36.8% with mixed $^{35}Cl-^{37}Cl$ or $^{37}Cl-^{35}Cl$, and 6% with $^{35}Cl-^{35}Cl$ isotopes.

3.1 Disordered Model

Applying the effective model (1) in the disordered case we consider the following values for the parameters of the corresponding eigenvalue equation (5). For the lattice sites with unit cells containing $^{35}Cl-^{35}Cl$ or $^{37}Cl-^{37}Cl$ we use the fitted values of E_0 given by eqs. (9) and (10), respectively. Since $E_0^{35-35}/E_0^{37-37} = \sqrt{37/35}$, as expected, we assume that for the lattice sites with mixed isotopes is

$$E_0^{mix} = E_0^{35-35}\sqrt{\frac{\mu_{35-35}}{\mu_{35-37}}} = 311\ cm^{-1}, \qquad (11)$$

where $\mu_{a-b} = \frac{ab}{a+b}$ is the reduced mass of a $^aCl-^bCl$ pair. As regards the hopping integrals J between adjacent unit cells, we use for the general case $^aCl-^bCl \rightarrow {}^{a'}Cl-^{b'}Cl$ the mean value $J^{a-b\rightarrow a'-b'} = \frac{1}{2}(J^{a-b} + J^{a'-b'})$, where the J^{35-35} and J^{37-37} are obtained from eqs. (9) and (10), and $J^{mix} = \frac{1}{2}(J^{35-35} + J^{37-37})$. Finally we use the same value $k = 1.2$ for each lattice site.

For the calculation of the fundamental Raman spectrum in this disordered case we consider a single quantum of excitation and calculate the energy distribution of the most localized eigenstates at the center of the lattice for a large number of different random configurations of the chloride isotopes. We assume that the most localized eigenstate is locally excited during the Raman process.

3.2 Numerical Method for the Calculation of the Spectrum

The Hamiltonian that is necessary to diagonalize in order to find the required energy distribution depends on the unknown eigenstate, since the last term of the right-hand side of eq. (5) −the nonlinear term− contains the corresponding wavefunction. We use an iterative numerical algorithm for calculating the most localized eigenstate at the center. This comprises the following steps:

i) choose a random configuration of $^{35}Cl-^{35}Cl$, mixed, or $^{37}Cl-^{37}Cl$ lattice sites, with the probabilities obtained from the natural abundance,

ii) start with a guess eigenstate completely localized at the center of the lattice,

iii) diagonalize the Hamiltonian and choose the eigenstate that is most localized at the central site,

iv) substitute the resulting eigenstate in the Hamiltonian and repeat the diagonalization,

v) if convergence is not achieved after a number of iterations of the order of 100-200, start again from step ii) and expand successively the central region of step iii) by including the two adjacent surrounding sites each time,

vi) when the algorithm converges, monitor the energy of the resulting eigenstate and repeat the procedure with another random configuration.

Typically, the percentage of convergence is more than 99%.

3.3 Fundamental Spectrum

The theoretical calculation of the fundamental spectrum as explained above yields a very good agreement [8] with the corresponding experimental results presented in reference [10]. In figure 3 we show the calculated spectrum in the case where the same weight is attributed to each eigenstate obtained from the algorithm described in

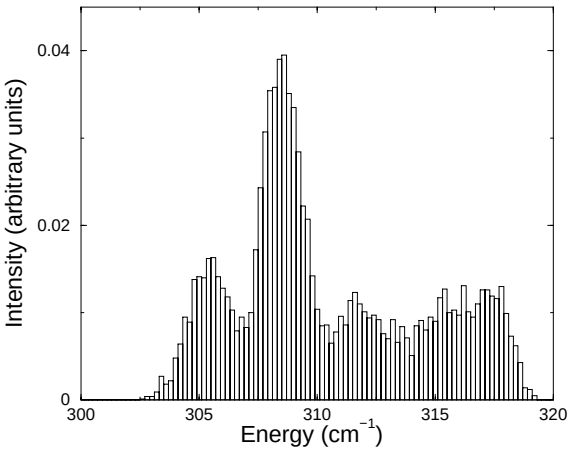

Figure 3: The energy distribution of the eigenstate which is most localized at the center of the lattice for naturally abundant $PtCl$. A Gaussian distribution of the on-site energies has been used for the broadening of spectral lines.

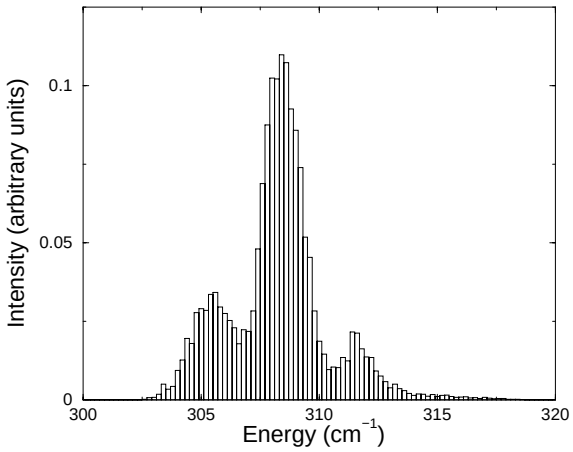

Figure 4: The calculated fundamental Raman spectrum of naturally abundant $PtCl$, taking into account an approximate Raman cross section of each eigenstate. We have again used a Gaussian distribution of the on-site energies.

the previous section. This spectrum exhibits a hump in the higher energy part that does not appear in the experimental profile. However, attributing a weight at each eigenstate of the disordered system obtained through a rough estimation of the Raman cross section [8], leads to the elimination of this structure. The corresponding spectrum is presented in figure 4.

In both figures 3 and 4 we have used 10^4 different random configurations of chloride isotopes and the convergence is 99.2%. Furthermore, a Gaussian distribution with variance $\omega_g = 0.6$ has been applied to the excitation energies (around their mean values ϵ_0 obtained through the parameters of section 3.1) in order to represent the finite width of the experimental spectra [8].

The model also describes accurately the positions of the peaks that appeared in the first overtone Raman spectrum [8]. In general the calculated spectra can accurately reproduce the energy of the spectral lines. Regarding the overall profiles, they slightly underestimate the intensity of the higher energy peak.

4 CONCLUSIONS

A simple phenomenological model in which the many-quanta intramolecular excitations corresponding to the symmetric stretching motion of the chlorides are linearly coupled to a bath of other degrees of freedom, represented by classical Einstein oscillators, is able to account for the localization of the vibrational energy and the resulting red-shifts that appeared in isotopically pure $PtCl$. The minimization of the total energy of this coupled system in the adiabatic limit yields a nonlinear eigenvalue problem for the N-quanta excitations. Through fitting of two parameters of the model an excellent agreement with the very large, experimentally observed relative red-shifts of the overtones is achieved. Without introducing any further parameters, the main features of the fundamental Raman spectrum of the natural abundant $PtCl$ are reproduced within the model, by taking into account an approximate estimate of the Raman cross section.

ACKNOWLEDGMENTS

We would like to acknowledge our collaborators A. P. Shreve, N. K. Voulgarakis and G. P. Tsironis. The research was supported by the Department of Energy under contract W-7405-ENG-36 and by the Los Alamos LDRD program.

REFERENCES

[1] B. I Swanson *et al.*, Phys. Rev. Lett. **82**, 3288, 1999.
[2] J. T. Gammel, A. Saxena, I. Batistic, A. R. Bishop, and S. R. Phillpot, Phys. Rev. B **45**, 6408, 1992.
[3] D. Baeriswyl and A. R. Bishop, Phys. Scripta **19**, 239, 1987; J. Phys. C **21**, 339, 1988.
[4] K. Kladko, J. Malek and A. R. Bishop, J. Phys.: Condens. Matter **11**, L415, 1999.
[5] T. Holstein, Ann. Phys. (N.Y.) **8**, 325, 1959.
[6] G. Kalosakas, S. Aubry and G. P. Tsironis, Phys. Rev. B **58**, 3094, 1998.
[7] N. K. Voulgarakis, G. Kalosakas, A. R. Bishop, and G. P. Tsironis, Phys. Rev. B **64**, R020301, 2001.
[8] G. Kalosakas, A. R. Bishop, and A. P. Shreve, *"Nonlinear disorder model for Raman profiles in naturally abundant PtCl"* (preprint).
[9] E. N. Economou, O. Yanovitskii, and Th. Fraggis, Phys. Rev. B **47**, 740, 1993.
[10] S. P. Love, L. A. Worl, R. J. Donohoe, S. C. Huckett, and B. I. Swanson, Phys. Rev. B **46**, 813, 1992.